JOURNAL OF APPLIED POLYMER SCIENCE VOL. 9, PP. 3071–3089 (1965)

Barus Effect in Filled Polymer Melts

SEYMOUR NEWMAN and QUIRINO A. TREMENTOZZI,
Monsanto Company, Plastics Division, Research Department, Springfield, Massachusetts

Synopsis

The influence of fillers on the post-extrusion swelling (Barus effect) of polymer melts is explored with the use of three model fillers in poly(styrene–acrylonitrile). The filler effect is shown to be more complex than simple dilution of the polymer. The role of such factors as melt rigidity, tendency toward plug flow, trapping of matrix in filler aggregates, and filler migration are considered.

INTRODUCTION AND BACKGROUND

The phenomenon of the expansion or puff-up of viscoelastic jets on emergence from capillaries (Barus effect) has evoked considerable attention from rheologists in recent years. The complexity of the phenomenon is now thoroughly appreciated. In addition to the fact that the parabolic velocity profile developed in the capillary must rearrange to a flat profile in the jet exterior to the tube, a variety of factors have been considered by many workers.[1–6] Various schools of thought have taken different approaches and one finds, therefore, treatments in terms of normal stresses developed inside the capillary and in the free jet, stored elastic energy, as well as molecular mechanisms based on polymer molecule orientation and deformation.

Qualitatively, we note that a crosslinked rubber forced from some reservoir through a capillary will recover from the imposed strain and return to its original shape on emergence from the capillary. Hence, it seems reasonable that for real polymer melts the effective elastic strain imposed on entering the capillary should depend on the rigidity of the elastic component and the stress level imposed by the experiment, in addition to the geometry of the capillary entrance. However, for the polymer melts of interest here, only temporary crosslinks (entanglements) exist, so that we may expect a decay of stress to occur as a result of any strain imposed by squeezing or extension flow from the reservoir into the capillary. It is no surprise, then, that at constant shear rate the jet diameter d_j, is found to decrease with increasing (L_c/D_c), the capillary length to diameter ratio, to some slowly changing or limiting value for long capillaries.

Bagley[7] has examined the puff-up as a function of increasing (L_c/D_c) and finds that, for polyethylene, (d_j/D_c) decreases exponentially with transit

time in the capillary. Most importantly, however, Bagley has shown that values of (d_j/D_c) for polyethylene, when extrapolated to infinite transit time, still show a dependence of stress. In this connection, let us compare the (d_j/D_c) values for poly(styrene–acrylonitrile) (S/AN) copolymers extruded from three capillaries of $(L_c/D_c) = 2$, 5, and 50 at 400°F. If the transit time, t_a, is taken as

$$t_a = \pi R^2 L_c/Q \tag{1}$$

where Q is the output rate, then equal transit times for the three capillaries will correspond to Newtonian shear rates at the wall, $\dot{\gamma}_{nw} = 4Q/\pi R^3$, which also stand in the ratio 2:5:50. Taking values at 30, 75, and 750 sec.$^{-1}$ for the three capillaries mentioned, we find (d_j/D_c) to be 1.50, 1.64, and 2.0, respectively. Clearly, in this system, too, the effective strain level, as characterized by (d_j/D_c), does not depend on transit time only, but on stress level or output rate, as well. Therefore, as a result of the above arguments, and from other considerations, it is believed that molecular chain orientation and deformation, induced by shear and extension flow at the capillary entrance or by shear alone in the capillary, will result in jet expansion of S/AN. Hence, even for long capillaries, in which entrance effects have largely decayed away, (d_j/D_c) should exceed one.

In the present report, it is our intention to discuss a particular aspect of the problem, i.e., the influence of fillers on the Barus effect in S/AN, as measured with relatively long capillaries. Only minor attention appears to have been given to this matter.[8,9] Because of the state of the science of viscoelasticity at this time, such a consideration cannot be entirely satisfying. Nevertheless, it should be possible to point out some of the important underlying factors contributing to the overall effect.

EXPERIMENTAL

Materials

Principal attention has been given to three fillers: commercial calcium silicate; an S/AN latex crosslinked with 0.625% divinylbenzene (DVB), and glass shot or beads. Approximate sizes of the fillers mentioned are indicated in Table I. All of these are essentially spherical except for the $CaSiO_3$, which has an asymmetry of about 10.

The S/AN matrices used for these fillers were preparations of $[\eta] =$ 0.7–0.8 as measured in methyl ethyl ketone at 30°C.

TABLE I

Filler	Average diameter, cm.
$CaSiO_3$[a]	12×10^{-4}
S/AN/DVB	10^{-4}–10^{-5}
Glass shot[b]	10–50×10^{-4}

[a] G. Cabot, Inc., Wollastonite P-1.

[b] Microbeads, Inc., Type MX-XL glass beads.

Sample Preparation

For the $CaSiO_3$ series, compositions were prepared so as to contain up to 0.5 volume fraction of the filler, ϕ_F, at 400°F. This corresponds to a maximum of 74.3 wt.-% at room temperature. Blending was achieved by 10 min. of mill rolling at 350°F., followed by cooling of the rolls to 220°F. and removal of the sample after an elapsed time of 20 min. The S/AN/DVB latices were blended with S/AN over a range of concentrations by extrusion. For this blend, the composition by weight corresponds closely to the composition by volume and was so treated. Glass beads were incorporated by mill rolling for 10 min. at 350°F. and were also prepared so as to have known volume fractions of filler at a temperature of 400°F., the temperature of rheological test.

Viscosity Measurement

Viscosity data were obtained with the Monsanto capillary extrusion rheometer (MCER) by using established procedures.[10] Capillaries of 0.05 in. diameter were used throughout. Crosshead speeds corresponding to shear rates of 3, 7.5, 15, 30, 75, 150, 300, 750, 1500, and 3000 sec.$^{-1}$ were generally employed. Unless otherwise stated, the apparent melt viscosity, η_a, was calculated at the wall without further correction by using the relations

$$\eta_a = \tau_w/\dot{\gamma}_{nw} \tag{2}$$

where τ_w is the shear stress

$$\tau_w = FD_c/\pi L_c D_p^2 \tag{3}$$

$\dot{\gamma}_{nw}$ is the Newtonian shear rate at the wall

$$\dot{\gamma}_{nw} = 2V_{XH}D_p^2/15D_c^3 \tag{4}$$

and F is force, D_c is capillary diameter, L_c is capillary length, D_p is plunger diameter, and V_{XH} is the velocity of the plunger.

Measurements of the Barus Index

There are several experimental factors which should be kept in mind which bear on the measurement of die swell. These include the following:
(*1*) effect of cooling to room temperature; (*2*) residual or frozen-in puff-up; (*3*) distribution of puff-up within the strand; (*4*) effect of gravity; (*5*) variation of die swell with distance from die exit.

The extruded strand draws under its own weight; efforts were made, therefore, to cut the extruded strand a short distance after extrusion. After cooling, the diameter of the cut strand, generally 1–3 in. in length, was measured at its thickest portion with a micrometer or hand microscope.

The diameter correction for shrinkage due to cooling $(\rho_s/\rho_m)^{1/2}$ the ratio of densities in the solid and melt states, is small and was neglected. An

attempt to assess the amount of "frozen-in" die swell was carried out by reheating the cooled extruded strands to about 350°F. for 15 min. No significant changes in dimensions were observed after this treatment, and it may be concluded from this and other studies that the time for the strand to achieve its full diameter was well within the time scale required for cooling of the strand.

It does not appear to have been pointed out that the observed extrudate swell must represent some average quantity reflecting the distribution of shear rates or shear stresses across the capillary. Taking, for instance, an area average of the shear stress, τ_A, for a capillary of radius R, we have

$$\tau_A = \int \tau dA/A \tag{5}$$

Since the shear stress in general is given by $\tau = \tau_w(r/R)$, where τ_w is the shear stress at the wall, and, since $dA = 2\pi r dr$, then

$$\tau_A = 2\tau_w/3 \tag{6}$$

The average shear rate for power-law fluids being a more complex function, it would appear desirable to correlate the Barus effect with an average shear stress such as τ_A. Since we have used capillaries of radius R of 0.025 in. exclusively, useful comparisons may be drawn from τ_w, which bears simple proportionality to τ_A. This, however, is not always convenient; therefore, when comparisons are made at fixed volumetric flow rates among melts which vary in velocity profile, this complication of averaging should be kept in mind. Also, for short capillaries where the effect of the capillary entrance is superposed on the shear flow in the capillary, the matter becomes more involved, and comparisons made at given values of $\dot{\gamma}_w$ or τ_w become obvious oversimplifications.

It should also be noted that the jet diameter requires a finite time to reach its equilibrium dimensions. This is discussed more fully in the Appendix. For this and other reasons discussed above, it was the custom to calculate the die swell (d_j/D_c) as the largest value observable in a given piece of cut strand.

Throughout, we have preferred to use as a measure of puff-up the quantity $(d_j/D_c)^2 - 1$, where d_j refers to the final extruded strand diameter. This has the characteristics of engineering strain as shown by the following simple argument; consider a cylindrical element of length $l(1 + \epsilon)$, in the capillary to be in a state of strain ϵ and with a volume $= \pi R^2 l(1 + \epsilon)$. After puff-up, the strain is relieved and the diameter increases from D in the capillary to d after puff-up.

Assuming no volume change,

$$(\pi D^2/4)l(1 + \epsilon) = (\pi d^2/4)l \tag{7}$$

hence,

$$\epsilon = (d^2/D^2) - 1 \tag{8}$$

RESULTS AND DISCUSSION

Melt Viscosity of Filled S/AN

The influence of different fillers on the concentration dependence of melt viscosity of S/AN at low shear rates is shown in Figure 1; data were obtained at 400°F. with $(L_c/D_c) = 50$. No attempt has been made to extrapolate the results to zero shear rate; instead, data gathered at 3.0 sec.$^{-1}$ were used directly.

Comparative data on the $CaSiO_3$, glass beads, and S/AN/DVB latex fillers show large disparities. The $CaSiO_3$ particles, being acicular in habit, induce the largest viscosity increase, as expected. An appropriate equation developed[11] for ellipsoids of axial ratio $1 < p < 15$ is

$$[(\eta_a)_F/(\eta_a)_0 - 1] = 2.5 + 0.4075(p - 1)^{1.508}\phi_F \quad (9)$$

For the particles of the type used here, this reduces to

$$[(\eta_a)_F/(\eta_a)_0 - 1] \simeq 12\phi_F \quad (10)$$

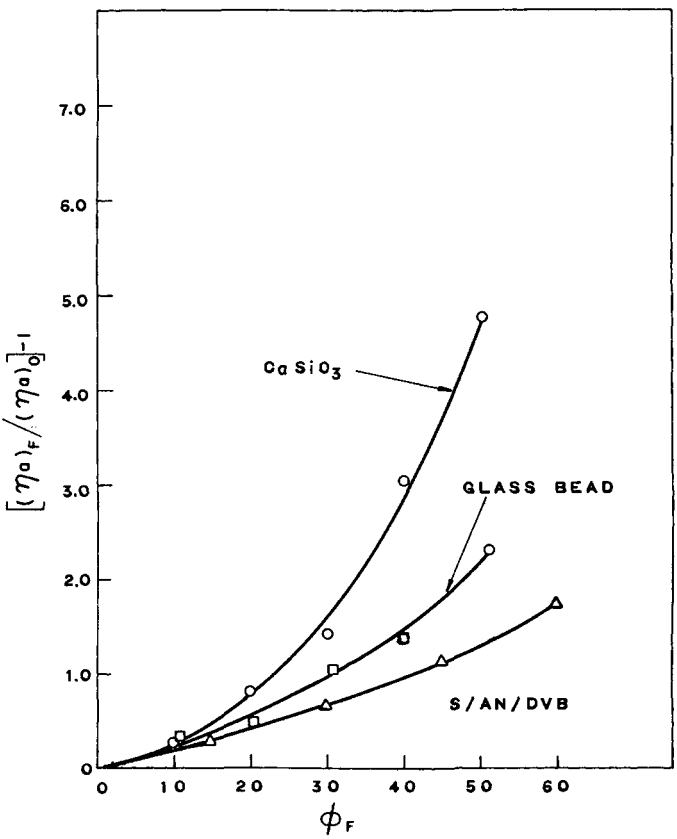

Fig. 1. Viscosity increment vs. volume fraction of fillers for high molecular weight ($[\eta] = 0.7$–0.8) S/AN with different fillers; $(L_c/D_c) = 50$, $T = 400$°F., $\dot{\gamma} = 3.0$ sec.$^{-1}$.

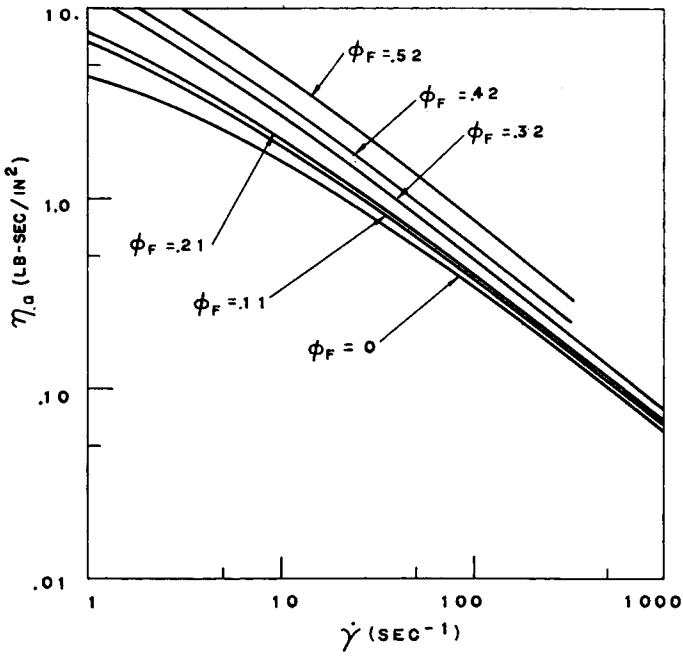

Fig. 2. Apparent melt viscosity vs. shear rate of S/AN filled with glass beads.

where the subscripts F and zero refer to the filled and unfilled systems, respectively. Such a relation does not, however, represent the data well over a broad concentration range. Many other relationships have been proposed, but we have not examined them for appropriateness.

The glass beads are seen to deviate from the simple Einstein relation with increasing concentration indicating strong interaction effects requiring the need for higher terms in the concentration. S/AN filled with the S/AN/DVB latex displays the weakest concentration dependence, suggesting that its deformability relative to the rigid glass particles is of significance in this respect.

As is well known, the apparent melt viscosity η_a of polymer melts is strongly shear-dependent. This is clearly shown by the plots of η_a versus the Newtonian shear rate at the wall $\dot{\gamma}_{nw}$ (Fig. 2). Of greater interest in the present context is the shear dependence of the filled composites. The data on the glass-filled system is presented as illustrative of the general results obtained: the filler is seen to have a noticeable effect on the shear-rate dependence of η_a with maximum divergence occurring at low shear rates. An inference which may be drawn from such data is that the velocity profile of flow within the capillary is altered by the filler, a matter which will be considered later in connection with the Barus effect.

For the needle-shaped $CaSiO_3$ particles, orientation of the long axis of the particles in the flow direction was revealed by interference microscopy on thin specimens taken from the surface of the strands where the shear rate

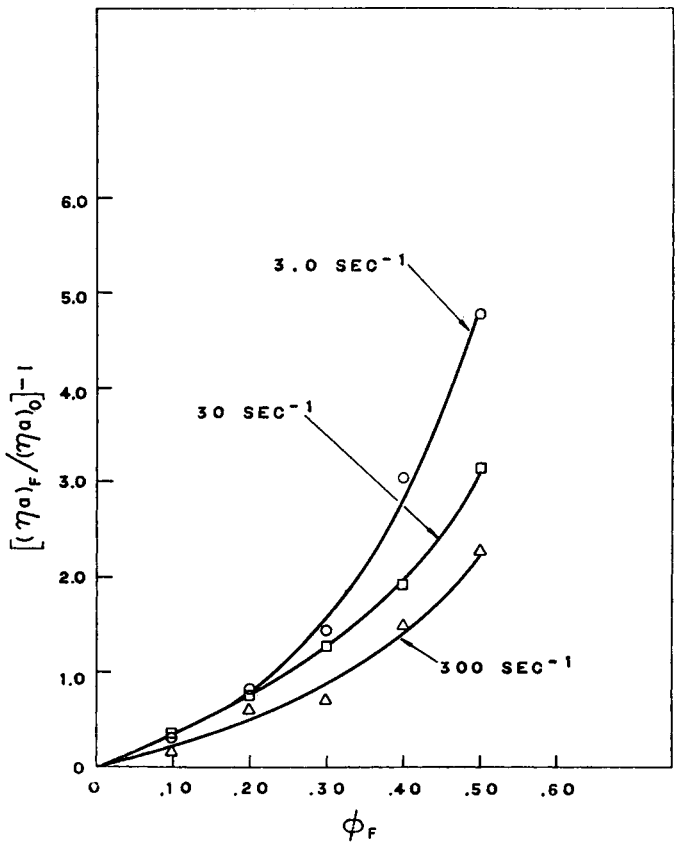

Fig. 3. Viscosity increment vs. volume fraction of calcium silicate in a high molecular weight S/AN ($[\eta]$ = 0.7–0.8) at different shear rates; (L_c/D_c) = 50, T = 400°F.

is at a maximum. The state of orientation in the strand interior has not been examined but presumably tends toward more randomness.

A decrease in the dependence of specific viscosity on filler content is disclosed with increasing shear rates (see Fig. 3, for instance). No studies were conducted to determine whether this was related to a breakdown with shear rate of particle aggregates.

Filler Effect in Post-Extrudate Die Swell of S/AN

Except for some brief studies concerning the end-correction and the influence of the (L_c/D_c) ratio on puff-up discussed later, this investigation on the influence of fillers on post-extrudate die swell was carried out almost entirely with relatively long capillaries of (L_c/D_c) = 50. Under these conditions, not only is the end correction to the apparent viscosity small, but since the transit time in the capillary is relatively long, the magnitude of the die swell approaches values which might be considered as infinite transit time values $(d_j/D_c)_{t=\infty}$ as calculated by Bagley from results with a

range of capillary lengths. Under these conditions, relaxation of effects due probably to the capillary entrance have largely decayed, and the observed post-extrudate swelling is believed to reflect largely the role of shear strain imposed by flow through the capillary itself.

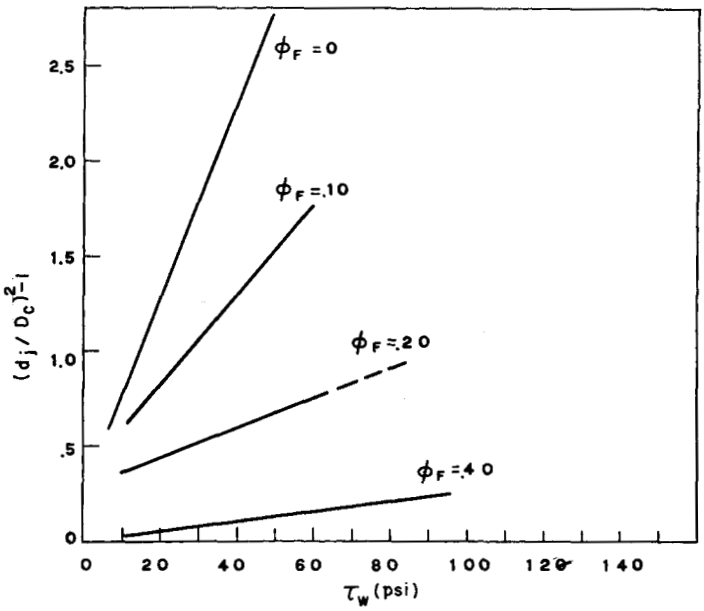

Fig. 4. Puff-up vs. shear stress for S/AN ($[\eta]$ = 0.7–0.8) filled with calcium silicate; (L_c/D_c) = 50, T = 400°F.

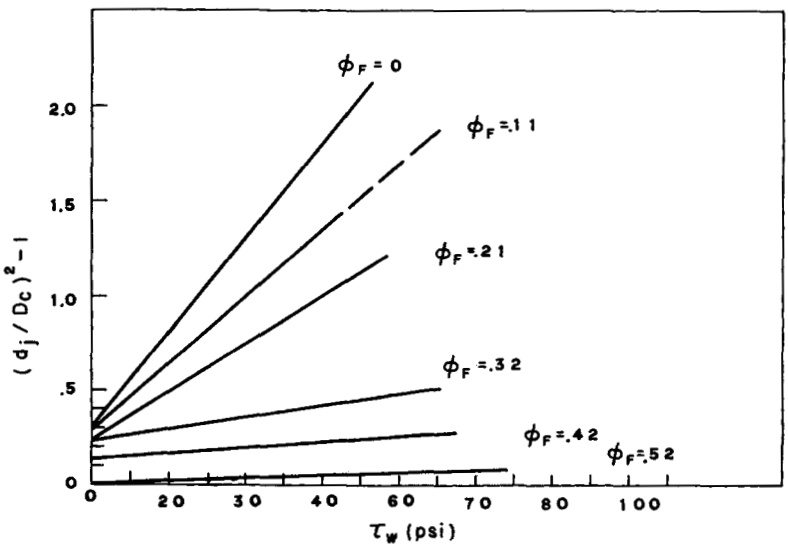

Fig. 5. Puff-up vs. shear stress for S/AN ($[\eta]$ = 0.7–0.8) filled with glass beads; (L_c/D_c) = 50, T = 400°F.

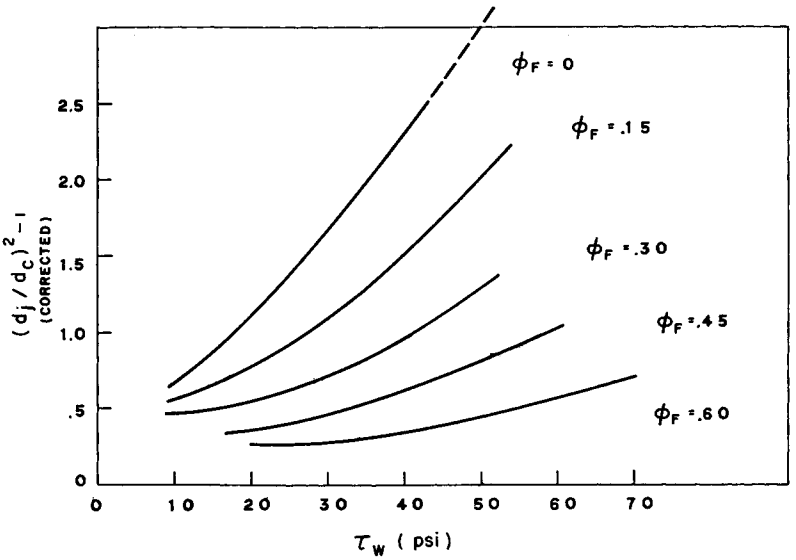

Fig. 6. Puff-up vs. shear stress for S/AN ([η] = 0.7–0.8) filled with S/AN/DVB; corrected for puff-up of filler; (L_c/D_c) = 50, T = 400°F.

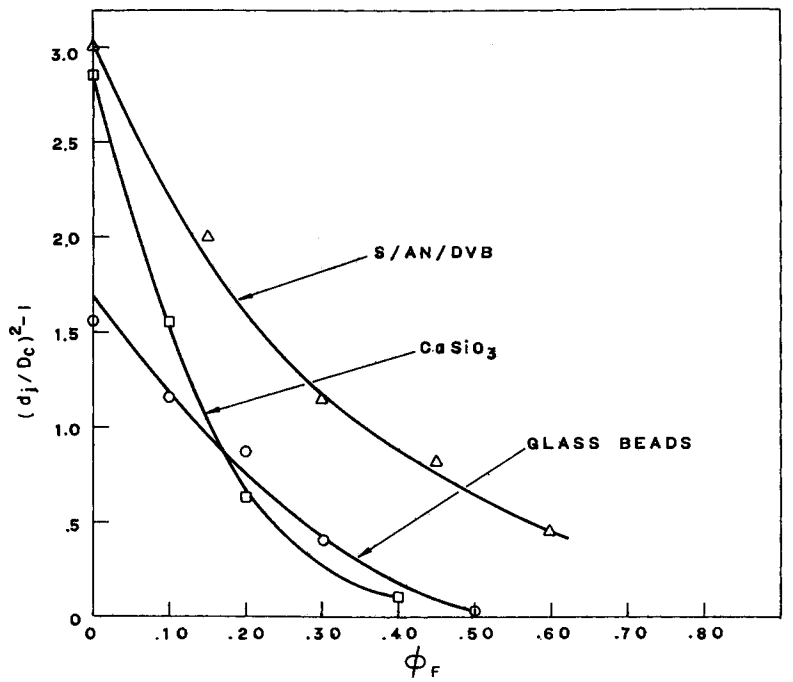

Fig. 7. Puff-up of filled S/AN ([η] = 0.7–0.8) vs. filler content; (L_c/D_c) = 50, T = 400°F.; τ = 50 psi.

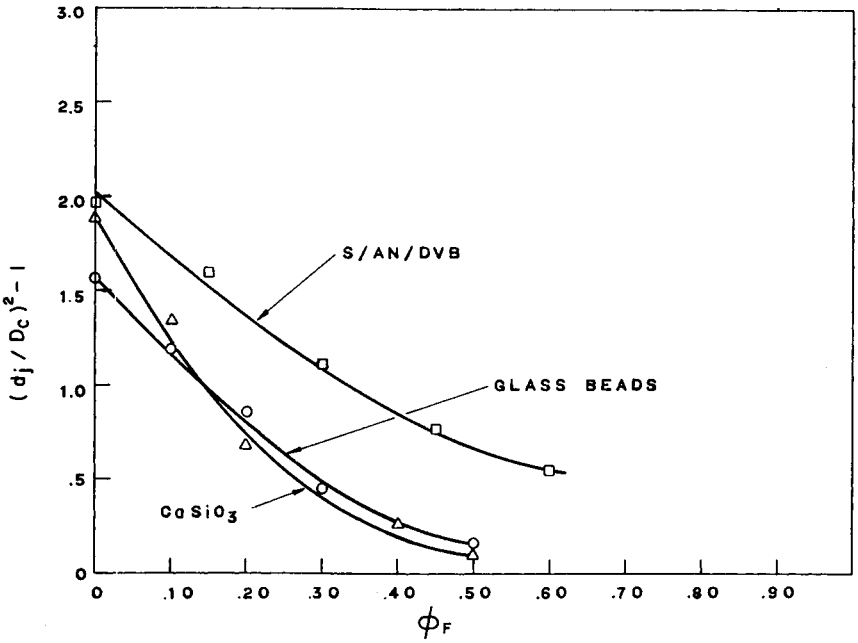

Fig. 8. Puff-up of filled S/AN ($[\eta]$ = 0.7–0.8) vs. filler content; (L_c/D_c) = 50, T = 400°F.; $\dot{\gamma}$ = 300 sec.$^{-1}$.

In agreement with Bagley's observations that $(d_j/D_c)_{t=\infty}$ increases with shear stress, the macroscopic strain, $(d_j/D_c)^2 - 1$ is seen to follow a nearly linear dependence on stress for the glass- and $CaSiO_3$-filled systems (see Figs. 4 and 5). In the case of the crosslinked latex filler, some curvature is noted (Fig. 6). However, in this instance the latex itself exhibits an appreciable die swell ($d_j/D_c \approx 1.4$), and it was necessary to subtract this factor in a manner proportional to its volume concentration in order to isolate the effect of the filler on the die swell of the matrix. The curvature shown in Figure 6 may reflect, therefore, the inexactness of this correction.

From these figures, it is evident that with increasing filler content the stress dependence of the die swell is diminished and approaches a limiting condition of zero dimensional changes on extrusion. It is entirely plausible that the puff-up (d_j/D_c) should approach one as the blend approaches pure filler which either exhibits no die swell or in the case of the S/AN/DVB latex has been subtracted out of the total.

However, data selected at either a fixed shear rate or shear stress and shown in Figures 7 and 8 clearly indicate a more rapid decline of die swell than simple dilution of the polymer would indicate. Assumption of $(d_j/D_c) = 1$ at the condition for close packing of spheres ($\phi_F \simeq 0.75$) does not alter this conclusion for the case of the glass beads. For the calcium silicate blends, where photomicrographic evidence exists of particle orientation (at least on the surface of the strand), it is not possible to estimate the condition of close packing.

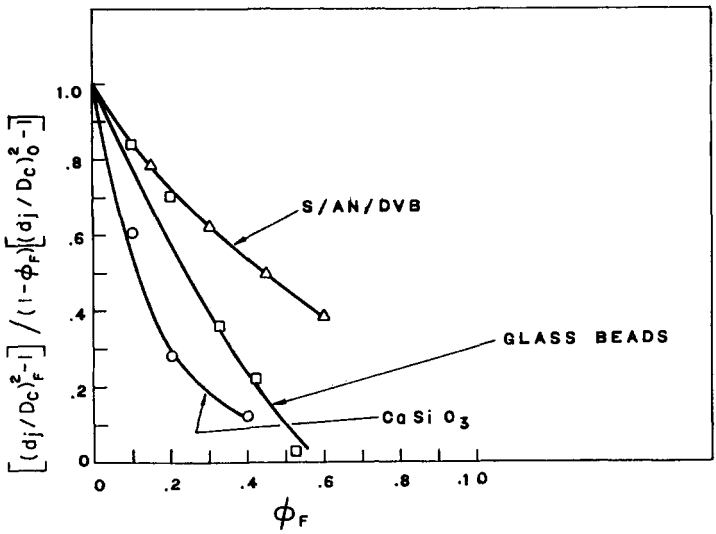

Fig. 9. Adjusted puff-up ratio vs. volume-fraction of filler for filled S/AN ($[\eta]$ = 0.7–0.8); (L_c/D_c) = 50, T = 400°F.; τ = 50 psi.

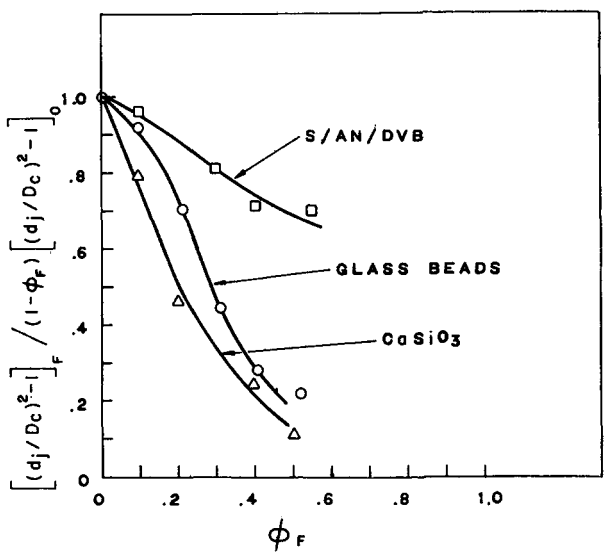

Fig. 10. Adjusted puff-up ratio vs. volume fraction of filler for filled S/AN ($[\eta]$ = 0.7–0.8); (L_c/D_c) = 50, T = 400°F.; $\dot{\gamma}$ = 300 sec.$^{-1}$.

The action of a filler in reinforcing a melt as revealed by an increase in the rigidity G' of polymeric melts is well established. Therefore, the data shown in Figure 7 at constant shear stress have been recalculated in the form of a ratio of strains $[(d_j/D_c)^2 - 1]_F/[(d_j/D_c)^2 - 1]_0$ for the filled and unfilled systems and have been also corrected by the factor $(1 - \phi_F)$ to equalize the polymer content in the filled and unfilled sample (Fig. 9).

On this basis, the ratio of strains at constant stress should, roughly speaking, be inversely proportional to the ratio of shear moduli. (The same data at constant shear rate are shown in Figure 10.) Increasing deviation from a horizontal line in Figure 9 might, therefore, correspond to increasing melt rigidity with concentration for the filled systems.

In the same connection, dynamic viscosity data of Takano,[12] for instance, reveal an increase of G' for polyethylene filled with spherical inorganic fillers. It is seen from this work that the magnitude of the increase of G' depends on the chemical nature of the filler, particle size, and concentration. Paralleling this effect, there is an increase of η', the real part of the dynamic viscosity. The magnitude of the increase of η', and of G' with ϕ_F, the volume fraction of filler, is shown by Takano to be roughly equivalent.

A glance at Figure 1 reveals that the viscosity increment increases in the order S/AN/DVB < glass beads < $CaSiO_3$. By analogy with Takano's data, we might again expect the increase of G' to be in the same order as the viscosity data. Unfortunately, we have no dynamic data on our systems to substantiate this conclusion. Insofar as this analogy is correct, however, it would appear that the magnitude of the filler effect on die swell as summarized in Figure 9 parallels the increase of melt rigidity in these systems.

In an attempt to provide some additional evidence for the relation of the filler effect and G', calculations of strain in sample viscoelastic models were performed. Values of G' were calculated for S/AN with about 0.3 volume fraction of glass beads from steady-state data according to the method described by Cox and Merz[13] and by utilizing the empirical expression

$$G' = \dot{\gamma}\sqrt{\eta_a^2 - \eta_c^2} \tag{11}$$

where η_a is the apparent viscosity calculated for this purpose from $\tau_{tw}/\dot{\gamma}_{tw}$ the ratio of the true shear stress at the wall and the true shear rate at the wall, and η_c is the consistency, $d\tau_{tw}/d\dot{\gamma}_{tw}$ or slope of the shear stress versus shear rate curve. For this calculation, values of τ_{tw} were calculated as described in the Appendix. $\dot{\gamma}_{tw}$ was obtained by applying the Rabinowitsch correction.[10]

Typical values of G' so obtained were 21 psi for the (S/AN)–glass composite at 15 $sec.^{-1}$ and 11 psi for the unfilled copolymer at the same shear rate. For a Voigt element subjected to a constant rate of strain, $\dot{\epsilon}$, the stress is given by the differential equation $\sigma = K\epsilon + \eta\dot{\epsilon}$, where η is the dashpot viscosity and K the spring constant.

Equating $\sigma = \tau_{tw}$, $K = G'$, and $\eta = \eta' = \eta_c$, Strella[14] derived the relation

$$\eta_a = \eta_c + G'/\omega \tag{12}$$

at ($\dot{\gamma} = a\omega$). On taking $a = 1$ and calculating the strain ϵ, values of about 0.7 were obtained for both the filled and unfilled S/AN.

Resort to a Maxwell element leads to about the same conclusions. Failure of such simple linear viscoelastic models to describe the experimental observations does not necessarily mitigate against the view that reinforce-

ment by the filler affecting an increase of G' is not a significant factor, but may only reflect the inadequacy of the models to fit the experiment and of the uncertainty in calculating G' from steady-state measurements.

Other Factors in Puff-up of Filled S/AN

Other factors related to melt reinforcement by fillers but having to do more directly with the matter of plug flow are: (*a*) velocity profile in the capillary; (*b*) particle migration toward the axis of the tube (tubular pinch effect); and (*c*) particle aggregation involving trapped matrix. Let us take these matters up in turn.

Velocity Profile for Steady Flow. It is well known that a parabolic velocity profile is characteristic of a Newtonian fluid. For pseudoplastic fluids the viscosity of the fluid is less at the tube wall than at the center and the parabola is flattened. McKelvey[15] cites instances where velocity profiles are plotted for different values of the exponent n in the following equation for power law fluids,

$$\eta_a = \eta^0 \left| \frac{\dot{\gamma}}{\dot{\gamma}^0} \right|^{n-1} \tag{13}$$

where η^0 and $\dot{\gamma}^0$ refer to a standard state. By utilizing this equation and the data shown in Figure 2, an average value of the parameter n has been calculated over the range of $\dot{\gamma}$ = 3–300 sec.$^{-1}$ for the system (S/AN)–glass beads with the results given in Table II.

TABLE II
Values of n in Equation (13) for the System (S/AN)–Glass Beads

Volume fraction of glass (nominal)	n[a]
0	0.35
0.1	0.31
0.2	0.30
0.3	0.26
0.4	0.24
0.5	0.24

[a] Average value calculated in the shear rate range of $\dot{\gamma}$ = 3–300 sec.$^{-1}$.

The parameter n is seen to decrease (greater pseudoplasticity) with increasing filler concentration and to correspond therefore to flatter velocity profiles.

It would seem possible from this sort of an analysis to construct an approach to the problem of puff-up by postulating a combination of shear and plug flow. While this is perhaps acceptable as a first approximation, it is complicated by the problem of axial migration of filler particles. This phenomenon has been observed in capillary flow of suspensions in low viscosity liquids[16,17] but does not seem to have been reported in polymer

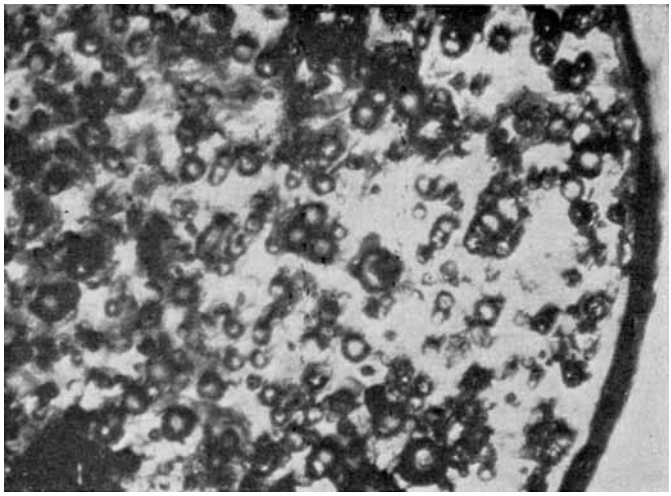

Fig. 11. Photomicrograph of cross section of extruded strand of polyethylene containing 30 wt.-% of glass beads; $T = 400°F.$, $\dot{\gamma} = 30$ sec.$^{-1}$.

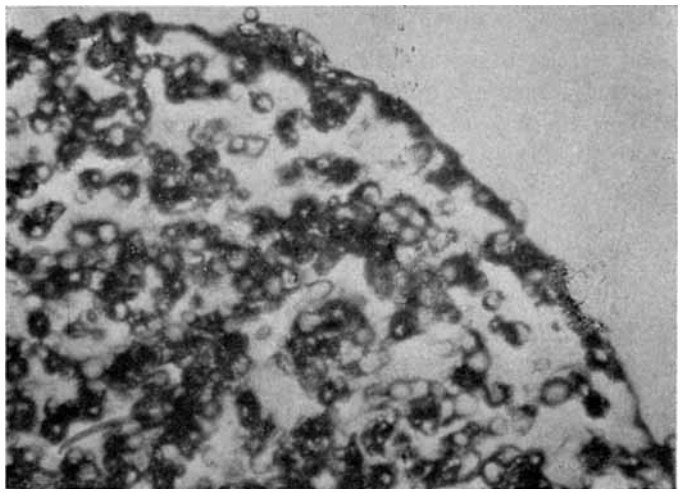

Fig. 12. Photomicrograph of cross section of extruded strand of polyethylene containing 30 wt.-% of glass beads; $T = 400°F.$, $\dot{\gamma} = 3000$ sec.$^{-1}$.

melts except that its occurrence is implied by observations on commercial extruded sheets.[18]

Axial Migration of Filler Particles. Blends of polyethylene and glass beads were extruded from the MCER and examined microscopically. Figures 11 and 12 show photographs of microtomed cross-sections of these strands. At low shear rates, the glass beads are seen to be aggregated but distributed throughout the body of the strand as well as near the surface. At high shear rates, aggregation is still evident but a layer of polymer relatively free of filler is disclosed near the strand surface.

The possibility that this axial migration is only apparent and arises as a result of puff-up may be discounted by the following argument. Consider the situation of a particle of radius r (see Fig. 13), at the wall in a capillary of radius R. Its relative position P is given by:

$$(R - r)/R = P \tag{14}$$

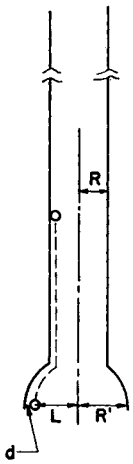

Fig. 13. Effect of puff-up on the position of a particle.

When the strand emerges and swells to a radius R', the particle remaining on a given streamline is still at the same relative position P which is now, however, given by

$$P = L/R' \tag{15}$$

The space d (Fig. 13) can be readily shown to be given by

$$d = r[(R'/R) - 1] \tag{16}$$

For filled systems, the die swell R'/R is generally less than 2, so that $d < r$. For particles the size of the glass beads (10–50μ), d is considerably smaller than the annulus of low filler concentration evident in Figure 12.

From the above observations it is to be noted, therefore, that there are two additional factors which may contribute to plug flow in the highly filled systems studied in this report: (*1*) the development of a zone of relatively low filler concentration at the surface which possesses a lower viscosity than the interior and (*2*) the formation of aggregates either stable or in dynamic equilibrium which temporarily trap or immobilize matrix polymer and thereby decrease the volume of material subjected to shear. These additional factors clearly contribute to the overall filler effect and serve to provide additional reasons for causing the post-extrudate die swell to decline with filler content more rapidly than by a simple dilution effect.

APPENDIX

End Correction and the Shear Modulus

In terms of the quantities used in experiments with the Monsanto capillary extrusion rheometer (MCER)[10]

$$\tau_{tw} = FD_c/A4(L_c + eD_c/2) \tag{17}$$

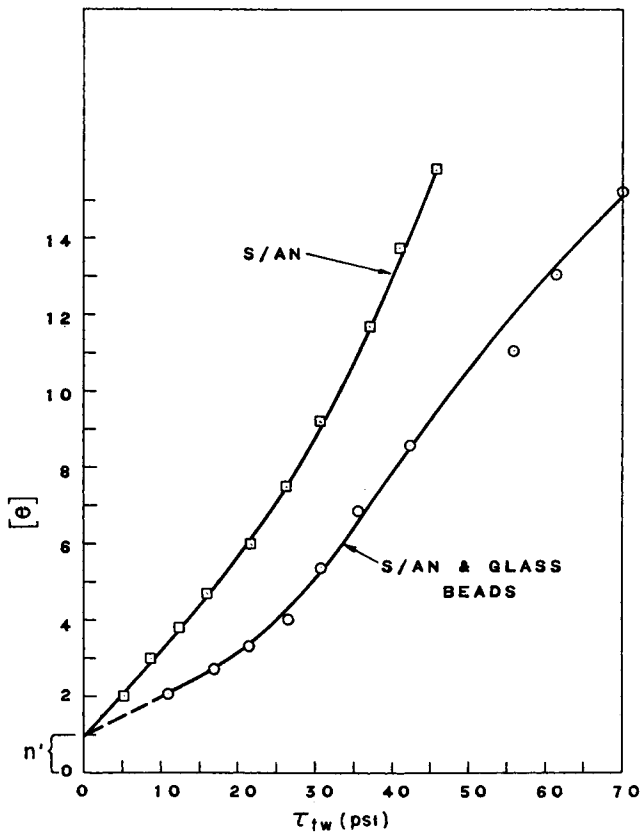

Fig. 14. End correction e vs. true shear stress at the wall for S/AN and S/AN containing 0.29 volume fraction of glass beads, T = 400°F.

where τ_{tw} = true shear stress at the wall, F is the force applied to the plunger, D_c and L_c are the capillary diameter and length, respectively, A is the cross-sectional area of the barrel, and e is an end correction[6,7] to the capillary length. A plot of F versus L/D at each shear rate leads to the intercept

$$2(L_c/D_c)_{F \to 0} = -e \tag{18}$$

and a slope of $4\tau_{tw}A$.

The quantity e has been interpreted[6,7] as

$$e = n' + (S_R/2) = n' + (1/2G')\tau_{tw} \tag{19}$$

where n' is a Couette correction, S_R a recoverable shear strain, and G' a shear modulus. Following established procedures, e was calculated from data obtained at each shear rate with capillaries of $(L_c/D_c) = 2$, 5, and 50. The observation[7] that e is linearly dependent on τ_{tw} for polyethylene is not substantiated by the present findings for the system S/AN (Fig. 14). This suggests that Hooke's law in shear is not obeyed in this system.

While in general e increases with shear stress and decreases with filler content in accord with the puff-up data obtained for this system, we hesitate to compare e with puff-up data quantitatively. The data recorded in Figure 14 and obtained with a long capillary of $(L_c/D_c) = 50$ probably reflects largely the molecular orientation taking place in the capillary and is expected to correlate with entrance effects but not to depend exactly on the same factors on which the treatment of e rests.

Relaxation Processes

Kinetics of Puff-up. Post-extrudate die swell does not occur instantaneously but requires a finite time or distance from the capillary face to develop its maximum value. Some brief efforts to establish a relation between strand diameter and distance beyond the die face were attempted by photographing the strand during extrusion from a simple melt-index type of apparatus. Strand photographs were taken by using a studio camera with a $f/16$ focal length, a xenon flash tube being used as a light source to illuminate both the sample and a transparent scale placed between the light source and the strand.

From photographs of the strand taken against the illuminated scale, values of the strand diameter d_j could be readily evaluated as a function of the distance y from the die face. This, together with information on the extrudate velocity, allows an evaluation of diameter versus time. It is evident that the decrease in length of the strand that accompanies puff-up or die swell does not permit a direct conversion of distance from the exit face of the die to time. In other words, the velocity of the extruded strand is influenced by the puff-up and shortening of the emerging polymer.

However, remembering that the flow volume is constant with respect to time, then at any point outside the capillary

$$\frac{A_c dy_c}{dt} = \frac{A_2 dy_2}{dt} = V_2 \tag{20}$$

$$\int_{t_0}^{t_2} dt = \frac{1}{A_c V_c} \int_{y=0}^{y=Y} A_2(y) dy \tag{21}$$

where A refers to cross-sectional area, V to velocity, and the subscript c to conditions in the capillary. From this, it can be shown that the time t

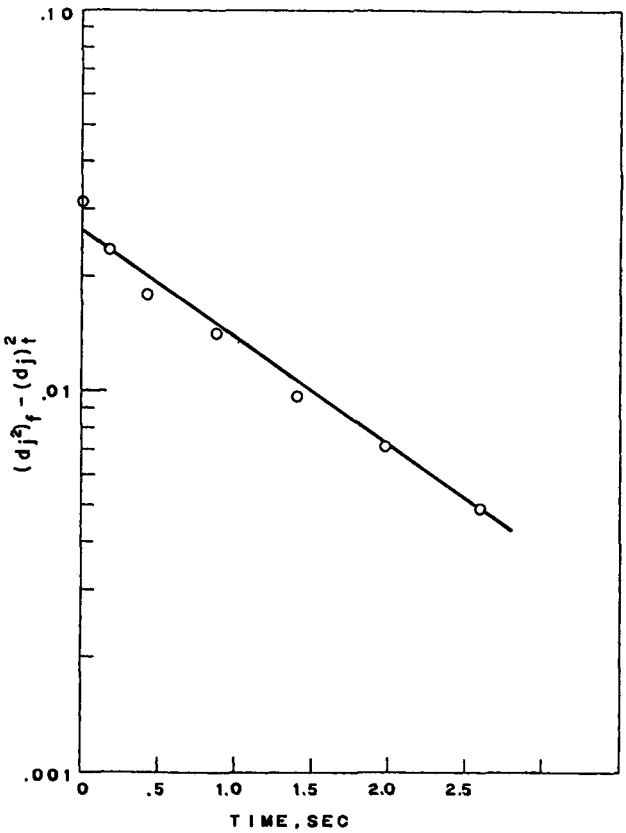

Fig. 15. Extrudate diameter vs. time for strands exiting from die at $T = 205°C$.

required to move from the capillary face, $y = 0$, to some coordinate position down-stream $y = Y$ where the cross-sectional area is $A_2(y)$ is given by

$$t \simeq A_2 Y / A_c V_c \simeq (d_j/D_c)^2 (Y/V_c) \tag{22}$$

Data of puff-up versus distance from the capillary exit obtained at 207°C. for a sample of S/AN was calculated from the photographs taken as described. Conversion of this to a time scale was carried out by using eq. (22) and is plotted in Figure 15 on a semilog coordinate scale. The resulting linear relation indicates that the strand of post-extrudate die swell is essentially exponential in time. Similar experiments carried out at 252°C. at about the same stress level (10 times the shear rate) shows an analogous behavior but with a faster approach to equilibrium probably as a result of the decreased viscosity of the melt.

The time scale for the quantity $(d_j/D_c)^2 - 1$ to reach half its maximum value is seen to be about 0.8 sec. at 205°C. Since this experiment involves both stress and strain recovery, it is difficult to relate this to fundamental quantities without an appropriate model.

It is with pleasure that we acknowledge the interest of Dr. D. Chappelear and the many helpful discussions we have had with him during the course of this work. We appreciate also the assistance given by him and S. Strella with certain calculations and the aid provided by A. Bibeau, W. Haugen, and J. Madden with some of the experimental work.

References

1. White, J. L., and A. B. Metzner, *Conference on Progress in International Research on Thermodynamics and Transport Processes, Princeton, 1962*, ASME, pp. 748–762.
2. Phillipoff, W., *Conference on Progress in International Research on Thermodynamics and Transport Processes, Princeton, 1962*, ASME, pp. 698–703.
3. Gavis, J., and S. Middleman, *J. Appl. Polymer Sci.*, **7**, 493 (1963).
4. Arai, T., and H. Aoyama, *Trans. Soc. Rheol.*, **7**, 333 (1963).
5. White, J. L., and A. B. Metzner, *Trans. Soc. Rheol.*, **7**, 295 (1963).
6. Phillipoff, W., and F. H. Gaskins, *Trans. Soc. Rheol.*, **2**, 263 (1958).
7. Bagley, E. G., S. H. Storey, and D. C. West, *J. Appl. Polymer Sci.*, **7**, 1661 (1963).
8. Hagan, R. S., and D. A. Davis, *J. Polymer Sci.*, **B2**, 909 (1964).
9. McCabe, C. C., and N. N. Mueller, *Trans. Soc. Rheol.*, **5**, 329 (1961).
10. Ballman, R. L., and J. J. Brown, *Capillary Rheometry*, Instron Engineering Corp., Canton, Mass.
11. Brodnyan, J. G., *Trans. Soc. Rheol.*, **3**, 61 (1959).
12. Takano, M., *Bull. Chem. Soc. Japan*, **37**, 78, 89 (1964).
13. Cox, W. P., and E. H. Merz, *J. Polymer Sci.*, **28**, 619 (1958).
14. Strella, S., *J. Polymer Sci.*, **60**, 59 (1962).
15. McKelvey, J. M., *Polymer Processing*, Wiley, New York, 1962, Fig. 3-2.
16. Segre, G., and A. Silberberg, *Nature*, **189**, 209 (1961).
17. Karnis, A., H. L. Goldsmith, and S. G. Mason, *Nature*, **200**, 159 (1963).
18. Giuffria, R., R. O. Carhart, and D. A. Davis, *J. Appl. Polymer Sci.*, **7**, 1731 (1963).

Résumé

On étudie l'influence des charges sur le gonflement après extrusion (effet Barus) des polymères fondus à l'aide de trois modèles de charges dans le poly(styrène–acrylonitrile). On montre que l'influence de la charge est plus complexe que la simple dilution du polymère. On considère le rôle de facteurs tels que la rigidité à l'état fondu, la tendance à l'écoulement visqueux, la fixation de la gangue dans les agrégats de charges, et la migration des charges.

Zusammenfassung

Der Einfluss von Füllstoffen auf das Nachextrusionsanschwellen (Barus-Effekt) von Polymerschmelzen wird mit drei Modellfüllstoffen an Poly- (styrol-acrylnitril) untersucht. Der Füllstoffeinfluss erweist sich als komplexer als einer einfachen Verdünnung des Polymeren entspricht. Die Rolle solcher Faktoren wie Schmelzsteifigkeit, Tendenz zur Propfenbildung beim Fliessen, Einschluss der Matrix in Füllstoffaggregate und Füllstoffwanderung wird in Betracht gezogen.

Received March 30, 1965